VORTEX STRUCTURES IN CIRCULAR PLATE HEAT EXCHANGERS

Tim Norden, Johann Turnow and Nikolai Kornev
Institute of Modeling and Simulation
University of Rostock
Albert-Einstein-Str. 2, 18059 Rostock
tim.norden@uni-rostock.de

ABSTRACT

Vortex structures and streamline patterns of turbulent flow in a single cross-corrugated channel of a circular plate heat exchanger have been investigated using RANS and hybrid URANS-LES methods. For validation simulations of a simplified plate heat exchanger model have been performed and compared to experimental data.

RANS simulations have shown that the fluid is homogeneously distributed over the circular plate due to the high flow resistance of the surface geometry. The flow structures gained by the hybrid model consist mainly of small eddies and large vortex tubes arising at the contact points. This leads to well mixing of the fluid.

INTRODUCTION

The use of plate heat exchangers is increasing over the past years. Based on their high performance and compact design they are replacing the conventional shell and tube heat exchangers. The thermo-hydraulic properties of plate heat exchangers depend strongly on the shape of the plate surface. High heat transfers rates reached due to elaborate plate designs, most often have to be paid for by high pressure losses. In the last century more than 60 different surface pattern for plate heat exchangers were developed (Shah & Focke (1988)). Today most surface geometries consist of the chevron geometry with a cross-corrugated surface pattern (Martin (2010)). In this case the plates are assembled being abutting in order that they contact in certain points. Between these contact points narrow and undulated flow passages are formed.

In the past many effort has been carried out to experimentally determine global heat transfer coefficients and overall flow losses to optimize hydrodynamic and thermodynamic properties of heat exchangers and to find empirical correlations to dimension them. Although it is known that the chevron geometry induces helical fluid flow in the narrow passages and vortex flow at the contact points, the influence of the complex three-dimensional flow on the heat transfer and the pressure loss is not well investigated. The structure of vortices created at the contact points is still an open issue and not completely understood.

The investigations published in literature point out that numerical simulations are taking more into account in the dimensioning process of heat exchangers due to the development of more powerful and more cost-effective computers. Bhutta *et al.* (2012) give a very good overview of the published literature in the means of numerical simulations of heat exchangers. It is shown that the RANS method is capable of calculating the performance of heat exchangers. In addition, Bhutta *et al.* (2012) state that the fields of interest can be divided into four branches: flow maldistribution, fouling, pressure drop and thermal analysis.

Kanaris *et al.* (2004) studied the pressure drop, the heat transfer and the fluid flow in a simplified model of a single channel of a heat exchanger. The channel consists of only one plate with a wave pattern keeping the model fairly simple. The results were in good compliance with experimental data and it was shown that CFD is a powerful tool for the calculation of plate heat exchangers. Despite that, Kanaris *et al.* (2004) observed that the fluid flow mainly follows the furrows of the corrugation profile until it is reflected at the side walls. This kind of fluid flow was also experimentally observed by Focke & Knibbe (1986).

The hydraulic performance of a real cross-corrugated single channel of a plate heat exchanger were numerically and experimentally investigated by Liu & Tsai (2010). The main focus of the authors was concentrated on the fluid flow behind the contact points, whereas heat transfer was neglected. They figured out that the fluid flow pattern differs in the developing area close to the ports and the fully developed area in the middle of the channel. In the developing area the fluid flow is separated at the contact points. One part follows the furrows until the next contact points and the other part follows the main flow direction. On the contrary, in the fully-developed region the fluid flow follows mainly the main flow direction behind the contact points.

Conclusively, the main focus of the investigations published in literature is pointed to calculate integral values of the fluid flow. Optimization by the means of CFD of the heat exchangers had not been done yet. Also, the physics of the development of vortices and their influence on pressure drop and heat transfer had not been studied. Therefore, the aim of this work is to study the fluid flow inside the narrow passages of a plate heat exchanger using time resolved numerical methods (LES/URANS) and to clarify the generation of vortices at the contact points and their influence on heat transfer. In future works the knowledge gained will be used to optimize the surface geometry of the plates.

A single channel of a circular plate-and-shell heat exchanger with a cross-corrugated surface pattern and a corrugation angle of 75°, as shown in Figure 1, is studied. Circular plate-and-shell heat exchangers are a new generation of heat exchangers which withstand higher internal pressures and higher temperatures due to their circular shape. Despite that, tube-and-shell heat exchangers in existing plants can be easily replaced by changing only the tube bundle with corrugated plates and keeping the old shell.

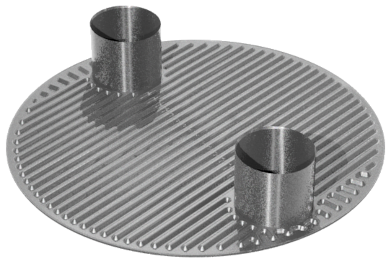

Figure 1. Single channel of the plate-and-shell heat exchanger.

COMPUTATIONAL METHODS

To determine the integral values of the single channel, simulations based on the Reynolds-Averaged-Navier-Stokes equations (RANSe) were performed using a 3-D finite volume method. For calculating unsteady effects and to determine the vortex structures a hybrid URANS-LES model proposed by Kornev *et al.* (2011) was used. Most plate heat exchanger plants are operated within the range of $200 < \mathrm{Re} < 2000$. The flow is treated fully turbulent in this work since in several publications it is stated that the flow regime in plate heat exchangers is already fully turbulent for Reynolds numbers in range of $200-650$ (Focke & Knibbe (1986), Vlasogiannis *et al.* (2002), Sha & Wanniararchchi (1991)).

In the hybrid URANS-LES model the near wall flow region is treated using URANS, whereas the far flow regions are treated using LES. Due to this, unsteady effects are taken into account and the number of grid nodes is lower than in pure LES. The model is based on the observation that the governing equations have the same form in URANS and LES (Kornev *et al.* (2011)).

$$\frac{\partial \bar{u}_i}{\partial t} + \frac{\partial(\bar{u}_i \bar{u}_j)}{\partial x_j} = -\frac{\partial \bar{p}^*}{\partial x_i} + \frac{\partial(\tau_{ij}^l + \tau_{ij}^t)}{\partial x_j} \tag{1}$$

The notation p^* is used for the pseudo-pressure and τ_{ij}^l and τ_{ij}^t for the laminar and turbulent stresses respectively. The turbulent stresses are calculated in dependency of LES or URANS region. The computational domain is dynamically divided into the regions depending on the ratio of the integral length scale L and the extended LES filter Δ. The integral length scale L is defined by Schlichting (2000).

$$L = 0.168 \frac{k^{3/2}}{\varepsilon} \tag{2}$$

The extended LES filter Δ is slightly modified from the proposal by Kornev *et al.* (2011).

$$\Delta = \sqrt{\frac{d_{max}^2 + \delta^2}{2}} \tag{3}$$

d_{max} is the maximal length of the cell edges $(\max(d_x, d_y, d_z))$ and δ is the standard LES filter width. If $L > \Delta$ the cell is in the LES region and if $L < \Delta$ the cell is in the URANS region, respectively. In Figure 2 the arrangement of the URANS and LES zones can be exemplary seen for a so called unitary cell of the plate heat exchanger.

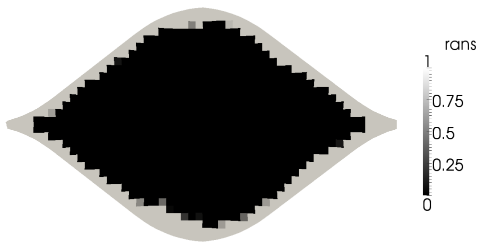

Figure 2. Unitary cell of a cross-corrugated pattern. Definition of URANS and LES zones in the hybrid model.

The Reynolds-stress tensor in the URANS region is modeled using the $k-\omega-$SST model proposed by Menter (1994). The subgrid stress tensor in the LES region is modeled using the dynamic Smagorinsky model proposed by Germano *et al.* (1991). For the discretisation of the governing equations in space and time a second order limited central difference scheme is used. Since the whole channel of the plate heat exchanger can only be simulated by using the RANS model due to restricted computational resources, only a small rectangular channel cut from the original model has been conducted for the hybrid model. The flow domain of the cut out channel is shown in Figure 3.

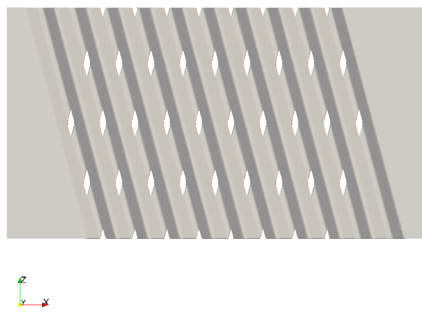

Figure 3. Rectangular cut out of the plate heat exchanger single channel for simulations with the hybrid model.

The surface geometry of the plate heat exchanger consists of many curves, contact points and sharp edges. Therefore the grid generation is fairly time consuming. Due to the complexity of the geometry, unstructured grids are generated. The generated grids consist mostly of hexahedron cells, but also prism and polyhedron cells were generated in regions of complex geometry. A special focus was paid to the inlet and outlet ports. In this region high velocity gradients occur due to the high decrease of the hydraulic diameter. A very fine mesh is needed to calculate these gradients correctly. For the single channel of the circular plate heat exchanger five different grids were generated in the cell size range from 3 million to 30 million cells. Grid independence check was performed to avoid numerical errors due to dependence of the results on the numerical grid. It was achieved for a grid with 18 million cells. For the rectangular channel also five different grids were generated with the number of grid nodes in the range from 2 million to 12 million cells. Grid independence was reached for a mesh with 8 million cells.

In both models in the inlet face Dirichlet boundary conditions were adopted for the velocity and the turbulent parameters, whereas Neumann boundary conditions were adopted for the pressure. In the outlet face, Dirichlet boundary conditions were adopted for the pressure, and Neumann boundary conditions for the velocity and the turbulence parameters. Ordinary no-slip conditions were used as hydrodynamic wall boundary conditions. In the rectangular channel a mapping plane was defined at a certain distance to the inlet. At this plane the velocity field was copied back to the inlet at every time step in order to get a fully developed velocity profile with correlated fluctuations in space and time.

RESULTS
Validation

For validation, grid independence and choice of RANS turbulent model simulations of turbulent flow in a simplified heat exchanger channel were conducted. The simplified model is represented by a rectangular channel, comprises of only one corrugated plate and a flat plate. Five different Reynolds numbers within the range $900 < Re < 1400$ have been considered, representing the flow regime in plate heat exchangers. The Reynolds numbers are based on the channel height which in this case is $0.01m$. Five grids with different numbers of grid nodes were investigated to establish grid independence. The first grid point is located at $y^+ = 0.3$ and several grid points are placed in the viscous sublayer. Therefore no wall functions are used for the turbulent closure models. The meshes are nearly homogeneous in every direction. Grid independence was achieved for a mesh with 1.7 million cells.

First the results for the pressure drop in the simplified channel are compared to the experimental and numerical results published by Kanaris *et al.* (2004). Figure 4 shows the Fanning friction factor f for different Reynolds numbers and turbulence models.

$$f = \frac{\Delta p d_h}{2\rho u^2 L_p} \tag{4}$$

The course of the simulated friction factor is for all turbulence models of hyperbolic shape, whereas the course of the experimental data is fluctuating. One explanation could be, that this occurred due to inaccuracies in the measurements. Therefore, the comparison between the numerical and experimental data in this case is not convincing. Nevertheless Table 1 shows the mean relative deviation of the numerical results to the experimental, respectively.

Secondly the results for the heat transfer are compared to experimental results published by Vlasogiannis *et al.* (2002) and the numerical results published by Kanaris *et al.*

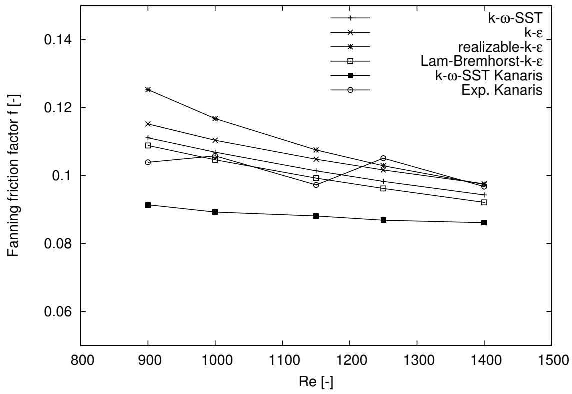

Figure 4. Flow in a simplified heat exchanger channel. Comparison of different turbulent RANS models and experimental data.

Table 1. Mean relative deviation of the numerical results to the experimental.

	Δf_{rel}	Δj_{rel}
k-ω-SST	0.0425	0.0228
k-ε	0.0543	0.0353
realizable k-ε	0.0886	0.0412
Lam-Bremhorst k-ε	0.0424	0.0218
k-ω-SST Kanaris et al.	0.1307	0.5209

(2004). The heat transfer is represented in terms of the j-Colburn factor and shown in Figure 5.

$$j = \frac{\mathrm{Nu}_m}{\mathrm{RePr}^{\frac{1}{3}}} \tag{5}$$

As it can be seen the course of the results is also of hyperbolic shape. The coincidence between numerical and experimental results is best for the k-ω-SST model by Menter (1994) and the Lam-Bremhorst k-ε model by Lam & Bremhorst (1981). The investigations of Zhang & Defu (2011) confirm these results. They had also detected that these models yield to the best results. For further investigations in this work the k-ω-SST was applied, because the simulations had shown that the Lam-Bremhorst k-ε model is computationally more expensive than the k-ω-SST model and is unstable in terms of convergence.

Integral values

Figure 6 shows the Fanning friction factor f for the single channel of the circular plate heat exchanger for different Reynolds numbers. The calculation of the hydraulic diameter and the mean velocity in the channel is based on the publication of Martin (2010). It can be seen, that the friction factor remains nearly constant with increasing Reynolds numbers. Thus, the pressure drop depends quadratically on the Reynolds number pointing to a high flow resistance in the channel due to the cross-corrugated pattern. This leads

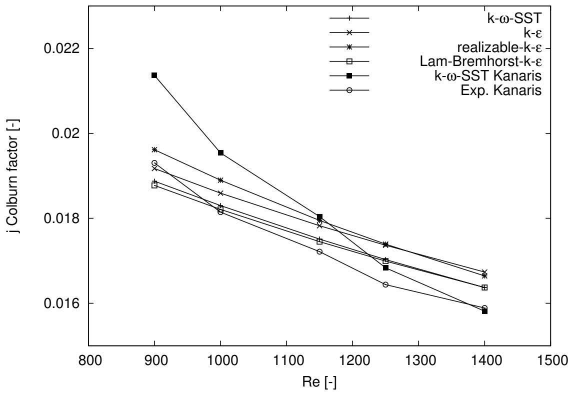

Figure 5. Flow in a simplified heat exchanger channel. Comparison of different turbulent RANS models and experimental data.

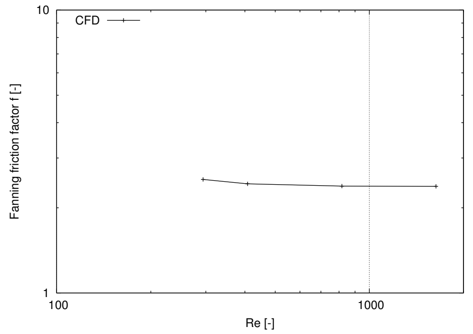

Figure 6. Flow in a single channel of a circular heat exchanger. Fanning friction factors for different Reynolds numbers.

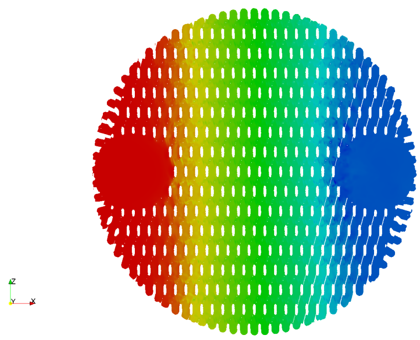

Figure 7. Flow in a single channel of a circular heat exchanger. Pressure distribution.

to a homogeneous distribution of the fluid over the whole plate, although the plate is circular. The pressure distribution is shown in Figure 7 and it can be seen that in the direction perpendicular to the main flow the pressure values are almost constant which leads to the understanding of a homogeneous distribution of the fluid.

After entering the channel, the fluid is separated at each contact point where one part follows the main flow direction. The other part is directed in lateral direction. Hence, no zones of nearly zero velocity could be observed. Only close to the inlet and outlet port blind areas with very small velocities are emerging due to the high flow rates. The main part of the fluid flow is driven through the narrow passages between the contact points. However, due to the contraction of the flow, the ratio of inlet velocity to maximum flow velocity between the corrugated plates can reach about $U/U_{inlet} = 31.58$.

To underline the results gained by numerical simulations, experimental investigations of the flow resistance being undertaken at the Technical University of Berlin at the moment. Despite that, flow visualizations will be carried out to prove the flow phenomena obtained by the numerical simulation.

Vortex structures

Focke & Knibbe (1986) published flow visualizations in cross-corrugated channels for different types of geometries. They showed that the flow pattern and the vortex structures strongly depend on the corrugation profile and on the corrugation angle. In this work the corrugation angle is 75° and the surface profile is nearly a sinusoidal pattern. For a sinusoidal profile and a corrugation angle of 80° Focke & Knibbe (1986) reported that the fluid does not only follow one furrow until it is reflected at the wall and enters the next furrow, but rather is reflected close to a contact point and the fluid is transported at this point from one furrow to another. These patterns can also be recognized in the streamline pictures (see Figure 8 and 9) averaged over $t^* = tU_b/L_p = 3$ of the hybrid URANS-LES simulation for the rectangular cut out channel of the plate heat exchanger model. Here, a proportion of the fluid follows the furrows and is reflected at the contact points as well. However, the main part of the fluid is driven through the narrow passages between the contact points in main stream direction, as mentioned before. Due to the shape of the heat exchanger plates, the fluid flows undulately through the passages.

Close downstream the contact points a counterflow is noticed inducing a relatively stable recirculation zone. In the downstream region between two contact points the fluid enters from both sides of the narrow passages from the main flow. Due to the evolving shear layer between main flow and recirculation zone vortex structures evolve. Thus, the the fluid is driven along spiral trajectories rotating around an inclined axis which drive the hot fluid back to the mean flow enhancing mixing process and heat exchange. The main part of the fluid ejected from the recirculation zone does not directly enter the following zone downstream. It is entrained by the main flow and hence becomes well mixed.

The streamline patterns barely depend on the Reynolds number. The patterns in Figure 8 and 9 are slightly different. At higher Reynolds numbers the recirculation zone behind the contact points is more distinct and thus, the rate of the fluid flow following the main stream flow is less. Based on this observation, it can be inferred that at higher Reynolds numbers the fluid is better mixed and distributed in the channel might resulting in higher heat transfer rates.

Figure 10 presents the vortex structures at Re = 1200 reconstructed by iso-surfaces using Λ_2 criteria which are colored by the global pressure. As it can be seen, the flow in the narrow passages is dominated by small scale eddies arising at the peaks and valleys of the latter. Whereas, in the region between the contact points the vortices are dominated by tubular and greater structures (see Figure 11) arising at the sharp edges of the contact points.

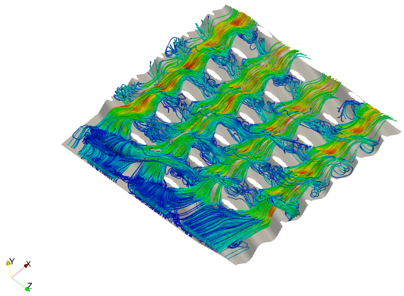

Figure 8. Streamline patterns for a rectangular cross-corrugated channel at Re = 400.

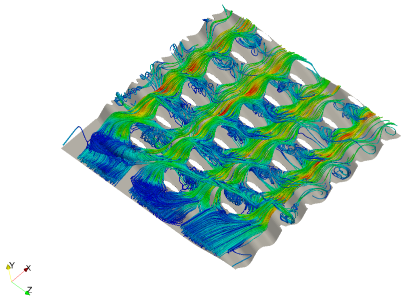

Figure 9. Streamline patterns for a rectangular cross-corrugated channel at Re = 1200.

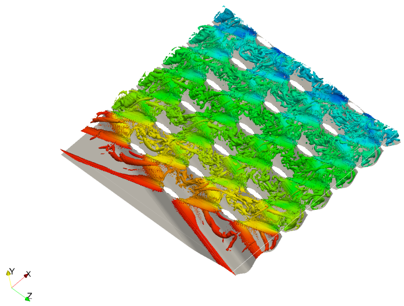

Figure 10. Visualization of vortex structures using λ_2-criterion for turbulent flow in a rectangular cross-corrugated channel at Re = 1200.

CONCLUSION

Numerical investigations have been performed for flow in a single channel of a circular plate-and-shell heat exchanger and in a rectangular cut out model of this plant. It was shown that the friction factor depends quadratically on the Reynolds number. Due to this high flow resistance the fluid is homogeneously distributed over the plate, although it is circular.

Despite that, it could be shown that the hybrid URANS-LES model by Kornev *et al.* (2011) is a powerful tool to predict vortex structures and unsteady effects without high computational costs. Streamline patterns showed that the flow in a cross-corrugated channel is characterized by large recirculation zones, disruptions and reattachments

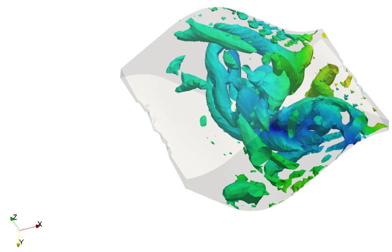

Figure 11. Visualization of vortex structures using λ_2-criterion for turbulent flow in a rectangular cross-corrugated channel at Re = 1200. Tubular vortex structures between the contact points in the downstream.

of boundary layers and vortex flow generation at the contact points which is in accordance with the experimental investigations by Focke & Knibbe (1986). This leads to a well-mixing of the fluid and thus to a high heat transfer rate. The flow consists mainly of small scale eddies, but at the contact points large eddies arise as well.

In future, the numerical results will be validated with experimental results of the integral values and flow visualizations which are being undertaken at the TU Berlin at the moment. In a next step the heat transfer between two or more channels will be simulated and the influence of the vortex structures on the heat transfer will be studied in more detail.

REFERENCES

Bhutta, M. M. A., Hayat, N., Bashir, M. H., Khan, A. R., Ahmad, K. N. & Khan, S. 2012 Cfd applications in various heat exchanger design: A review. *Applied Thermal Engineering* **32**, 1–12.

Focke, W. W. & Knibbe, P. G. 1986 Flow visualization in parallel-plate ducts with corrugated walls. *J. Fluid Mech.* **165**, 73–77.

Germano, M., Piomelli, U., Moin, P. & Cabot, W. H. 1991 A dynamic subgrid-scale eddy viscosity model. *Physics of Fluids* **3**, 1760–1765.

Kanaris, A. G., Mouza, K. A. & Paras, S. V. 2004 Designing novel compact heat exchangers for improved efficiency using a cfd code. In *1. International conference: From scientifing computing to computational engineering*.

Kornev, N., Taranov, A., Shchukin, E. & Kleinsorge, L. 2011 Development of hybrid urans-les methods for flow simulation in the ship stern area. *Ocean Engineering* **38**, 1831–1838.

Lam, C. K. G. & Bremhorst, K. A. 1981 Modified form of the k-ε model for predicting wall turbulence. *Journal of Fluids Engineering* **103**, 456–460.

Liu, F. & Tsai, Y. 2010 An experimental and numerical investigation of fluid flow in a cross-corrugated channel. *Heat Mass Transfer* **46**, 585–593.

Martin, H. 2010 Pressure drop and heat transfer in plate heat exchangers. *VDI Heat Atlas* pp. 1515–1521.

Menter, F. R. 1994 Two-equation eddy-viscosity turbulence models for engineering. *AIAA Journal* **32**, 1598–1605.

Schlichting, H. 2000 *Boundary layer theory*. Springer.

Sha, R. K. & Wanniararchchi, A. S. 1991 *Industrial Heat*

Exchangers, chap. Plate heat exchanger design theory. von Karman Institute Lecture Series.

Shah, R. K. & Focke, W. W. 1988 *Plate Heat Exchangers and Their Design Theory*, pp. 913–932. Hemisphere Publishing, New York.

Vlasogiannis, P., Karagiannis, G., Argyropoulos, P. & Bontozoglou, V. 2002 Air-water two-phase flow and heat transfer in a plate heat exchanger. *International Journal of Multiphase Flow* **28**, 757–772.

Zhang, L. & Defu, C. 2011 Turbulence models for fluid flow and heat transfer between cross-corrugated plates. *Numerical Heat Transfer, Part A: Applications* **59**, 267–296.